Irradiation of nitrogen rich ices by swift heavy ions

Clues for the formation of ultracarbonaceous micrometeorites

B. Augé^{1,2,*} E. Dartois², C. Engrand³, J. Duprat³, N. Bardin³, M. Godard³, L. Delauche³, H. Rothard¹, P. Boduch¹, A. Domaracka¹, C. Mejia^{1,5}, R. Martinez^{1,4}, G. Muniz¹

- Centre de Recherche sur les Ions, les Matériaux et la Photonique CIMAP, Boulevard Henri Becquerel, BP 5133 14070 Caen Cedex 05, France (CEA/CNRS/ENSICAEN/Université de Caen Basse Normandie)
- ² Institut d'Astrophysique Spatiale, UMR 8617 CNRS-Univ. Paris-Sud, Université Paris-Saclay, Bâtiment 121, Univ. Paris-Sud, 91405 Orsay Cedex, France
- ³ Centre de Sciences Nucléaires et de Sciences de la Matière, UMR 8609 CNRS/IN₂P₃-Univ. Paris-Sud, Université Paris-Saclay, Bâtiment 104, 91405 Orsay Campus, France.
- ⁴ Departamento de Física, Universidade Federal do Amapá, Brazil
- ⁵ Departamento de Física, Pontifícia Universidade Católica, Rio de Janeiro, Brazil

Received ...

ABSTRACT

Context. Extraterrestrial materials, such as meteorites and interplanetary dust particles, provide constraints on the formation and evolution of organic matter in the young solar system. Micrometeorites represent the dominant source of extraterrestrial matter at the Earth's surface, some of them originating from large heliocentric distances. Recent analyses of ultracarbonaceous micrometeorites recovered from Antarctica (UCAMMs) reveal an unusually nitrogen-rich organic matter. Such nitrogen-rich carbonaceous material could be formed in a N₂-rich environment, at very low temperature, triggered by energetic processes.

Aims. Several formation scenarios have been proposed for the formation of organic matter in UCAMMs. We experimentally evaluate the scenario involving high energy irradiation of icy bodies subsurface orbiting at large heliocentric distances.

Methods. The effect of Galactic Cosmic Ray (GCR) irradiation of ices containing N_2 and CH_4 was studied in the laboratory. The N_2 - CH_4 (90:10 and 98:2) ice mixtures were irradiated by 44 MeV Ni^{11+} and 160 MeV Ar^{15+} swift heavy ion beams at 14 K. Similar ice compositions have been observed at the surface of some icy bodies in the outer solar system. The evolution of the samples was monitored using *in situ* Fourier transform infrared spectroscopy (FTIR). We follow the column density of the initial ice molecules and of new species formed by radiolysis as a function of projectile fluence. After irradiation, the target is annealed to room temperature. The solid residue of the whole process left after ice sublimation is characterized in situ by infrared spectroscopy, and the elemental composition measured ex-situ. One of the samples was further annealed to 300 $^{\circ}$ C under vacuum and characterized by FTIR.

Results. The infrared bands appearing during irradiation allow to identify molecules and radicals (HCN, CN $^-$, NH $_3$, ...). The infrared spectra of the solid residues measured at room temperature show similarities with that of UCAMMs. The agreement is even better when the residue has been post-annealed to 200-300 °C under vacuum. The results point toward the efficient production of a poly-HCN like residue from the irradiation of N $_2$ -CH $_4$ rich icy bodies surfaces. The room temperature residue provides a viable precursor for the organic matter found in UCAMMs.

Key words. Astrochemistry, Oort Cloud, Cosmic rays, Meteorites, meteors, meteoroids, Methods: laboratory: solid state

1. Introduction

Interplanetary dust particles (IDPs) and meteorites provide information about primitive Solar System matter and its chemical evolution. Micrometeorites (AMMs) recovered in Antarctic snow, near the CONCORDIA station (Duprat et al. 2007) or near Dome Fuji (Nakamura et al. 1999; Ebihara et al. 2013) provide a unique source of pristine interplanetary dust particles. Among the fraction of AMMs that underwent a minimal weathering at atmospheric entry, a few percent of them are characterized by a very large carbon content (Nakamura et al. 2005; Duprat et al. 2010). The carbonaceous phase of the so-called ultracarbonaceous Antarctic micrometeorites (UCAMMs), is an organic matter that exhibit extreme deuterium excesses (Duprat et al. 2010). These particles are different from classical IDPs and AMMs and represent a new class of interplanetary material (Nakamura et

al. 2005; Duprat et al. 2010; Dobrică et al. 2011, 2012; Yabuta et al. 2012; Engrand et al. 2015). Analysis by Raman and infrared absorption spectroscopy of these UCAMMs (Dartois et al. 2013; Dobrică et al. 2011) revealed that the organic matter of UCAMM is nitrogen-rich. The spectra of these UCAMMs are different from that of insoluble organic matter (IOM) extracted from carbonaceous meteorites. The formation of such organic matter requires a specific nitrogen-rich low temperature environment, and a significant source of energy. These conditions may be encountered at the surface of some objects beyond the trans-Neptunian region with N2-rich icy surfaces. The energy can be provided by cosmic ray and VUV photon irradiation. Different scenarios have been proposed to explain the formations of UCAMMs in Dartois et al. (2013). UCAMMs may be (1) a heritage from the protoplanetary disk, (2) a fragment from a large Kuiper Belt object (KBO), or (3) a residue of irradiated ices formed on a comet-parent body in the Oort Cloud. However,

^{*} send offprint requests to basile.auge@ganil.fr

the macromolecular residues formed according to the first irradiation scenario should be different in composition from that found in UCAMMs (Dartois et al. 2013). Indeed due to the presence of abundant water ice in protoplanetary disk and dense interstellar environments, the matter recovered should present some features related to a higher amount of incorporated oxygen atoms in the solid network, whereas the organic matter of UCAMMs exhibit a low O/C ratio. In the last two scenarios (2,3), the formation of nitrogen-rich organic matter in the outermost regions of the Solar System can be explained, since nitrogen and methane rich ices are condensed at the surface of icy bodies, and water ice is buried and protected from the ambient radiation fields. These scenarios are favored to explain the formation of N-rich organic matter, both by the expected final organic matter composition and the volume of irradiated material. However, experimental constraints on irradiation times corresponding to these locations in the Solar System (e.g. Cooper et al. 2003) and on the volume of matter affected are needed to better distinguish the most fitting scenario. The third scenario allows the largest affected volume, combining a region where icy bodies are exposed to higher energy cosmic rays penetrating deeper in the subsurface, and with potentially more small icy bodies with a N2-CH4 rich subsurface than in the second scenario.

Several publications have reported experimental studies on ion bombardment of interplanetary ice analogues with N_2 and CH_4 included in the mixture (e.g. Gerakines et al. 2004; Moore et al. 2003; Hudson et al. 2001). These experiments were mainly performed at low ion energies, less than a few MeV. Here, we report on the effect of swift heavy ions corresponding to GCR (Galactic Cosmic Ray) irradiations of a typical large KBO or Oort Cloud icy body surface, and discuss the astrophysical implications for the formation and evolution of the organic matter observed in UCAMMs.

2. Experiments and methods

2.1. Experiments

The irradiation experiments were performed at the heavy ion accelerator "Grand Accélérateur National d'Ions Lourds" (GANIL, Caen, France) with Ni¹¹⁺ (44 MeV) at the IRRSUD beam line and Ar¹⁵⁺ (160 MeV) at the SME beam line. The experimental procedures have been reported before (Pilling et al. 2010; Seperuelo Duarte et al. 2009). The CASIMIR set-up ("Chambre d'Analyse par Spectroscopie Infrarouge des Molécules IRadiées", Figure 1) which can be mounted on both of these beam lines, is a high vacuum chamber ($\sim 10^{-8}$ mbar) with a rotatory platform holding an IR transparent ZnSe substrate. The latter can be cooled down with a closed-cycle helium cryostat to a temperature of about 14 K, allowing a controlled substrate temperature from 14 K to 300 K. The irradiation beam lines are equipped with a beam sweeping device, which provides an homogeneously irradiated surface. In the present experiments, we condensed a gaseous mixture of N2 and CH4 onto the ZnSe substrate at 14 K. We used two N₂-CH₄ mixtures, the first one with a nominal concentration of 1.99% of methane (98:2) and the second one with 9.98% (90:10). Both were acquired from Air Liquide and used as received (see Table 1). Such mixtures are representative of the main composition for methane and nitrogen-rich surfaces of the dwarf planet Pluto (Cruikshank et al. 2015) and are also relevant for some surfaces on dwarf planets (e.g. Eris, Makemake - Licandro et al. 2006; Lorenzi et al. 2015). Thousands of smaller objects in the Kuiper Belt and Oort cloud regions should possess the same kind of surface composi-

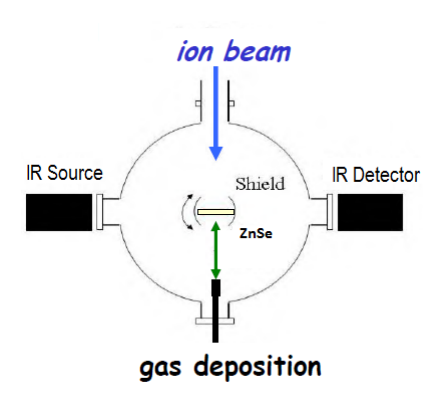


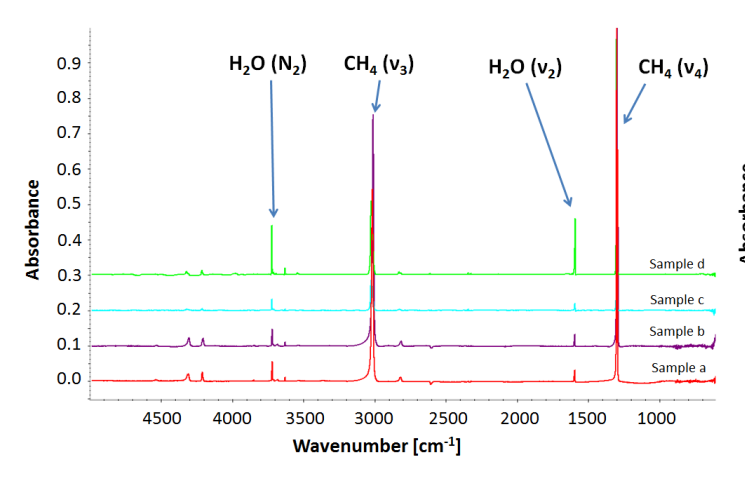
Fig. 1. Experimental set up CASIMIR. The gas is injected and condensed on a ZnSe window. This window can be rotated to be exposed to the ion beam or to the Fourier Transformed Infrared (FTIR) beam.

tion, but their spectra are not yet accessible due to their too low magnitudes. The substrate on the cold head can be rotated into three positions, to deposit the ice, to irradiate it or to record IR absorption spectra at normal incidence. Spectra were recorded in situ with a FTIR spectrometer (Nicolet Magna 750) before and during irradiation at different fluences, and at different temperature steps during heating. The slow warming-up was performed from 14 K to 300 K with a ramp at ~ 0.2 K min⁻¹ for $T \le 70$ K (to allow a gentle non processed N_2 and CH_4 sublimation) and with a 1-1.5 K min⁻¹ ramp for T > 70 K. When the sample reached 300 K, a final IR spectrum was recorded. The chamber was then opened to dismount the ZnSe window covered with the residue. The residue was kept under primary dry vacuum for further ex situ analysis. Electron microprobe measurements (Cameca SX100) were performed at the Pierre and Marie Curie University (Paris VI, CAMPARIS) at 10 kV in order to measure the atomic N/C ratio of the residues. One of the residue was also post-annealed under primary vacuum up to 300 °C to observe the evolution of the organic matter composition, as monitored by FTIR. The residue was placed under dynamic primary vacuum in an evacuated quartz tube placed into an oven, and the temperature raised to 600 K (300 °C) at 5 K min⁻¹. The sample is maintained at 600 K during 30 minutes and then removed from the oven. The sample is allowed to cool down under vacuum at room temperature before any further measurement.

2.2. Ice samples

Figure 2 presents the spectra of four different deposited N_2 -CH₄ ices. Two of them (sample a and sample b) were prepared with the (90:10) mixture with a thickness of 8.4 and 9.9 μ m, respectively. The others (sample c and sample d) were prepared with the (98:2) mixture with a thickness of 10 and 20 μ m, respectively. The thickness has been determined using residual interference fringes measured on the IR spectra as summarized in Table 1. The IR spectra of freshly deposited ice films (Fig.2) reveal different absorption bands at 4550, 4310, 4210, 3010, 2820 and 1305 cm⁻¹ which can all be assigned to the CH₄ molecule (Gerakines et al. 2005). Other bands observed at 3720, 3635 and 1600 cm⁻¹ correspond to small amounts of water residual pollution trapped into the N₂ matrix (Bentwood et al. 1980) whereas N₂ is IR inactive. This water comes from a residual gas contamination in the injection chamber.

The deposited ice column density can be calculated as



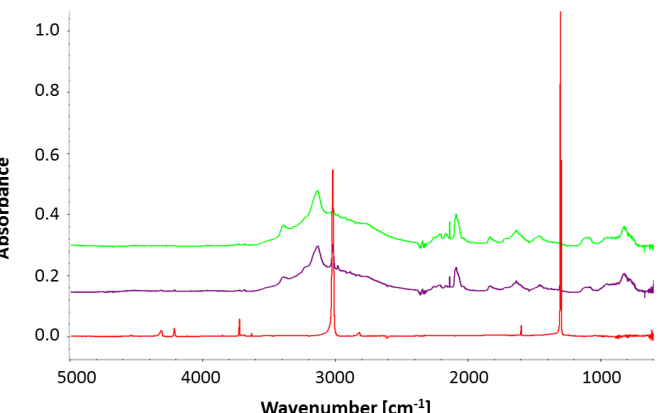


Fig. 2. IR spectra of samples a to d. Sample a and b were deposited using a (90:10) N₂-CH₄ mixture, sample c and d using a (98:2) mixture. Spectra were shifted for clarity. Small amounts of water contamination are present in the spectra. The major bands are identified, see text and Table 1 for details.

$$N = \frac{1}{A} \int_{\nu_1}^{\nu_2} \tau(\nu) \, d\nu \tag{1}$$

where N is the column density in molecules.cm $^{-2}$, $\tau(\nu)$ the frequency dependent optical depth of the considered infrared band and A the integrated band strength in cm.molecule $^{-1}$. The band strengths we adopted for the different molecules can be found in Escobar et al. (2014), Moore et al. (2003) and Gerakines et al. (2005). The effective initial composition is obtained using the methane band at 3010 cm $^{-1}$ and the water band at 1600 cm $^{-1}$ as reference. The adopted band strength values are $A_{CH_4}=6\times10^{-18}$ and $A_{H_2O}=1.2\times10^{-17}$ cm.molecule $^{-1}$, respectively. Table 1 summarizes the mixtures composition for the deposited ice films, the estimated sample thickness, the molecules column densities, taking into account the presence of H_2O .

The two ice films with 10% of methane (sample a and b) were irradiated with Ni¹¹⁺ at 44 MeV and the ice films with 2% of methane (sample c and d) with Ar¹⁵⁺ at 160 MeV. The beam parameters are given in Table 1. The samples have been irradiated until a total fluence of 1.0×10^{13} , 3×10^{13} , 3.4×10^{12} and 2.2×10^{13} ions cm⁻² was reached, for samples a to d, respectively. The total dose deposited in the ices (given in Table 1) have been calculated using the SRIM code (Ziegler et al. 2010), assuming an ice density of 0.94 g.cm⁻³ (Satorre et al. 2008).

3. Results

3.1. Irradiation of the ice mixtures

Infrared spectra taken before, during and at the end of the irradiation for the four samples are shown in Figures 3, 4, 5 and 6. These spectra clearly show the decrease of the CH₄ bands related to the destruction of this molecule under irradiation. Figure 6 exhibits a strong water ice contamination at the end of the experiment as shown by the broad water ice bands around 3280 cm⁻¹ and 1600 cm⁻¹. For this particular sample, the beam was stopped during 12 hours due to a technical incident, and an important layering of water ice occurred on top of the N₂-CH₄ film.

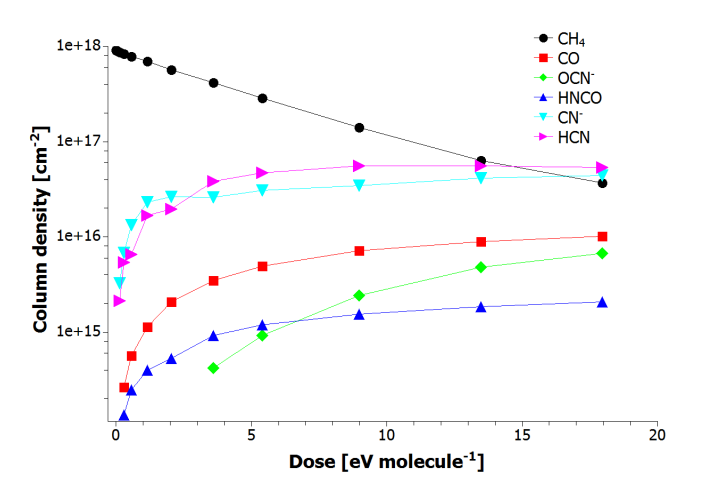


Fig. 3. (top) Sample a: IR spectrum from 5000 to 600 cm⁻¹ of $N_2{:}CH_4{:}H_2O$ (9.4 μm thickness). From bottom to top, initial deposited ice sample (red) , after a fluence of 5×10^{12} ions cm⁻² (purple) and 1×10^{13} ions cm⁻² (green). The final dose is 18~eV molecule⁻¹. Spectra have been shift for clarity. (bottom) Evolution of the column density of selected molecules in the sample during the irradiation as a function of the deposited dose.

Nevertheless the experiment was pursued immediately to the last fluence when the beam was recovered. It is worth mentioning that the water-ice deposition occured at the surface of the ice mixture, whereas the irradiation affected the bulk sample.

Numerous molecules can be formed as a result of the radiolysis of CH₄, N₂ (and H₂O). For high CH₄ concentration, molecules such as C₂H₆ are formed, as demonstated by the features at 2975, 2950 and 2890 cm $^{-1}$. The production of NH₃ (1640 and 1100 cm $^{-1}$) or NH₄⁺ (1470 cm $^{-1}$) is due to the destruction of N₂ combined with the one of CH₄ or H₂O. The production of small amounts of CO (2140 cm $^{-1}$), CO₂ (2345 cm $^{-1}$), HCNO (2260 cm $^{-1}$), OCN $^{-}$ (2170 cm $^{-1}$) are resulting from the small water ice contamination which is the only source of atomic oxygen in the ice mixtures. The feature around 2100 cm $^{-1}$ can be assigned to the formation of the CN $^{-}$ anion (2090 cm $^{-1}$) and HCN (2100 cm $^{-1}$). This molecule is also present at 3130, 1730 and 820 cm $^{-1}$.

The evolution of the column density of the most relevant molecules as a function of the deposited dose is reported in Figures 3, 4, 5 and 6, and the infrared bands used to evaluate the column densities are listed in Table 2. In these figures after about 10 eV molecule⁻¹, the column densities of the main species do

Table 1. Table of deposited molecules

Sample	Conc.a	Thickness ^b	Molecule ^c	N^d	Beam	Energy	S_e^{-e}	Fluence	$Dose^f$
	N ₂ :CH ₄	$[\mu \mathrm{m}]$		$[cm^{-2}]$		[MeV]	[keV μ m ⁻¹]	[ions cm ⁻²]	[eV molecule ⁻¹]
a	90:10	8.4 ± 0.4	CH ₄	1.7×10^{18}	⁵⁸ Ni ¹¹⁺	44	3794	1.0×10^{13}	18
			H_2O	1.6×10^{16}					
b	90:10	9.9 ± 0.5	$\mathrm{CH_4}$	1.5×10^{18}	⁵⁸ Ni ¹¹⁺	44	3794	3.0×10^{13}	54
			H_2O	1.6×10^{16}					
c	98:2	10 ± 0.6	$\mathrm{CH_4}$	2.6×10^{17}	$^{40}Ar^{15+}$	160	1617	3.4×10^{12}	3
			H_2O	8.3×10^{15}					
d	98:2	20 ± 2	$\mathrm{CH_4}$	6.3×10^{17}	$^{40}Ar^{15+}$	160	1617	2.2×10^{13}	18
			H_2O	4.4×10^{16}					

^a Concentration given by Air Liquide; ^b The thickness is estimated from the interference fringes period via the formula e≈1/2nΔν, e is the thickness, n the refractive index of the ice film, and Δν the period of interference fringes; ^c Taking into account the water pollution; ^d The calculated water contamination is about 1-7% with respect to CH₄; ^e Calculated with SRIM (Ziegler et al. 2010), assuming an ice density of 0.94 g cm⁻³ (Satorre et al. 2008); ^f D = F × S_e/ρ, where F is the ion fluence, S_e its electronic stopping power and ρ the target density.

not further evolve substantially. This suggest that after such a dose the abundances of the irradiation-induced molecules reach a plateau although the sample still evolve toward a refractory residue as seen through the presence of broad bands in the IR spectra. We can also notice that the initial composition does not significantly change the overall chemical evolution (Figure 3, 4 and 6). The final spectra starting with a 2% or a 10% methane ices are similar (see sample a, b and d on Figures 3, 4 and 6). To infer the relevance of the dose deposited in the ices, sample c has been exposed to a total dose of only about 3 eV molecule⁻¹ (Figure 5). The final spectra shows that the complex features around 3010 cm⁻¹ and 2200-2000 cm⁻¹ are much lower than in other experiments, i.e. that the final dose is not sufficient to radiolyse enough CH₄ and N₂ to produce higher molecular weight species (see Figure 5). The methane's column density evolution shows that at the end of the irradiation a substantial fraction of the initial methane is still present in the ice.

Table 2. List of formed molecules or radical ions, only the most intense band is given for each species.

	- 4/ D	-
Molecule	Band (cm ⁻¹)	Reference
HCN	2100	Burgdorf et al. (2010)
C_2H_6	2975	Bennett et al. (2006)
$C_2H_4N_4$	2210	Gerakines et al. (2004)
NH ₃	1100	Pilling et al. (2010)
CO	2140	Palumbo et al. (1993)
HNCO	2260	Jheeta et al. (2013)
NH₄ ⁺	1470	Moon et al. (2010)
CN ⁻	2090	Moore et al. (2003)
OCN-	2170	van Broekhuizen et al. (2004)

Table 3. Infrared absorption bands observed in the residue formed after irradiation, and their attribution.

Bands	Attribution
3500 - 2400 cm ⁻¹	N-H
2200 cm ⁻¹	C≡N
1650 cm ⁻¹	C=C
1600 cm ⁻¹	C=N
1350 cm ⁻¹	C-N

3.2. Annealing of irradiated ices to 300 K : formation of organic residues

After each irradiation, the samples were slowly heated from 14 K to 300 K (annealing) to sublimate the ices and examine the residue. At the beginning, the temperature ramp was chosen to be slow enough (0.2 K min⁻¹) to allow for gentle diffusion and sublimation of the matrix and avoid explosive desorption of the ice matrix when nitrogen and methane sublimate (e.g. volcano effect).

For T \geq 70 K, the ramp was increased to 1 or 1.5 K min⁻¹. During annealing, infrared spectra were recorded to monitor the chemical evolution of the sample. The corresponding spectra in the 2300-2000 cm⁻¹ region are shown in Figures 7 and 8 for the four samples.

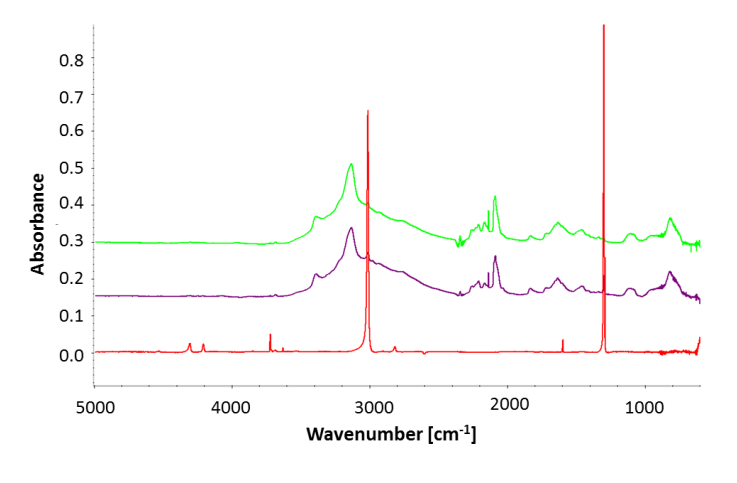
The first species that sublimates is CO, as demonstrated by the disappearence of the 2140 cm⁻¹ band beyond 35 K. CH₄ and N₂ also sublimate around this temperature. Once the matrix has evaporated, as the temperature increases, strong modifications related to the band complex between 2200 and 2050 cm⁻¹ are still observed. The CN⁻ and HCN bands disappear progressively and the band complex evolves toward higher frequencies corresponding to nitrile and isonitrile transitions in a solid residue.

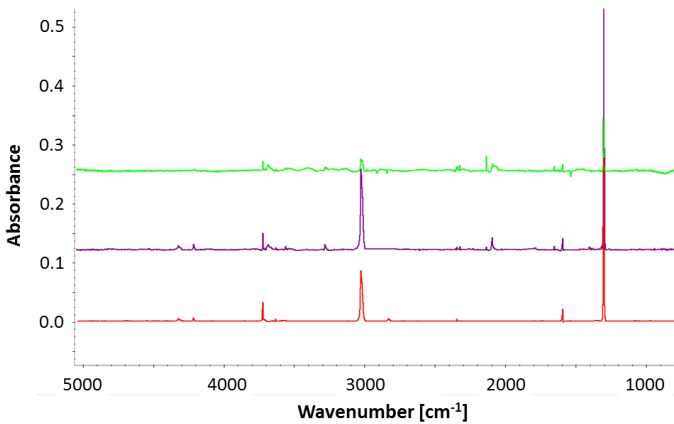
Although sample c was irradiated at a lower total dose (3 eV molecule⁻¹), the residue IR spectrum is similar to the ones obtained for higher doses. This shows that even at such low dose a residue is already formed, although thinner.

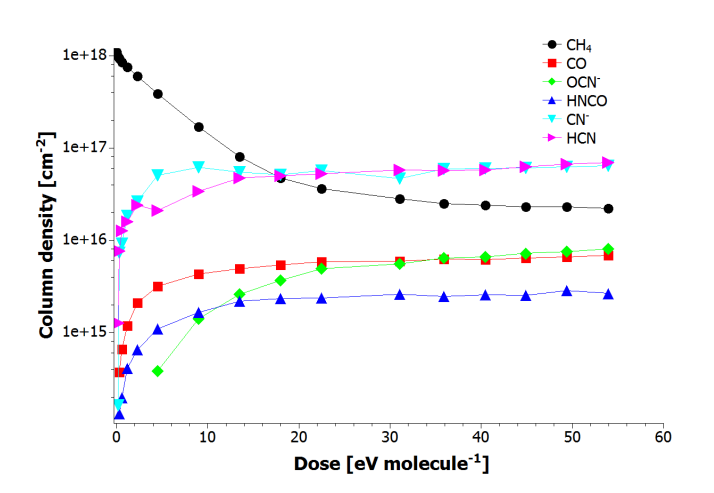
The final spectra indicate that even if the evolution of the spectra are different and even if the initial composition are slightly different, the residues are similar.

The absorbance of the N-H feature between 3500 cm⁻¹ to 2400 cm⁻¹ increases with the final dose deposited during the irradiation. The same evolution is observed in the nitrile region at 2200 cm⁻¹. However, in the region of C=C, C=N and C-N (at 1650 cm⁻¹, 1600 cm⁻¹ and 1350 cm⁻¹), the most intense spectra are that of sample b and d followed by sample a and c.

The spectra of the room temperature residues of sample a, b, c and d are shown in Figure 9. The spectrum of residue d, after heating to $600~\rm K~(300~^{\circ}C)$ under primary vacuum, is displayed in the same figure. The main bands identified in the residue are reported in Table 3.







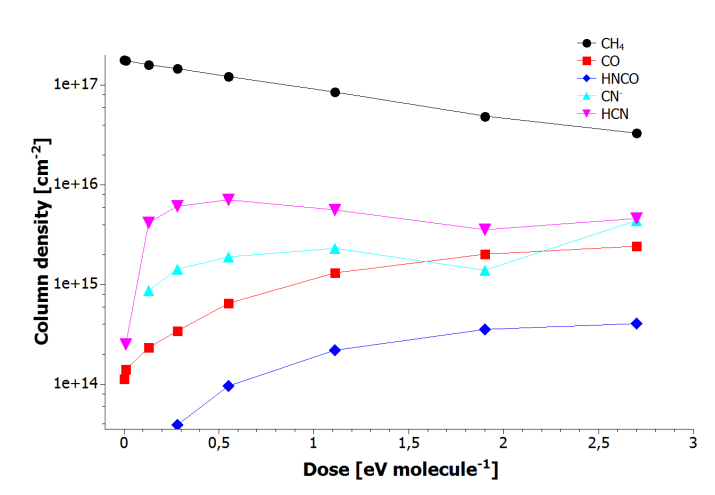


Fig. 4. (top) Sample b: IR spectrum from 5000 to 600 cm⁻¹ of N_2 :CH₄:H₂O (9.2 μm thickness). From bottom to top, initial deposited ice sample (red) , after a fluence of 1×10^{13} ions cm⁻² (purple) and 3×10^{13} ions cm⁻² (green). The final dose is 54 eV molecule⁻¹. Spectra have been shift for clarity. (bottom) Evolution of the column density of selected molecules in the sample during the irradiation as a function of the deposited dose.

Fig. 5. (top) Sample c: IR spectrum from 3700 to 700 cm⁻¹ of N₂:CH₄:H₂O (9.3 μ m thickness). From bottom to top, initial deposited ice sample (red), after a fluence of 6.9×10^{11} ions cm⁻² (purple) and 3.4×10^{12} ions cm⁻² (green). The final dose is 3 eV molecule⁻¹, not enought to obtain a final spectra equivalent to those of other samples irradiated with higher doses. Spectra have been shift for clarity. (bottom) Evolution of the column density of selected molecules in the sample during the irradiation as a function of the deposited dose.

4. Discussion

4.1. Residue formation

Although starting with different initial concentrations and depositing different final doses, the produced residues share similar spectral signatures.

Figure 9 shows the similarity between a spectrum from Gerakines et al. (2004) obtained after an irradiation of pure HCN ice and the four residue spectra of this work.

Indeed, the pure HCN residue presents the same features as listed in Table 3. Moreover, the nitrile band presents the same intensity as that of the residues obtained in this work. This indicates that, as shown in Figures 3, 4, 6 and 5, one of the most abundant molecules formed during irradiation is HCN and CN^- and that other molecules present before annealing are contributing less significantly to the residue. Swift heavy ions transform an $N_2\text{-}CH_4$ ice in a HCN polymer compound.

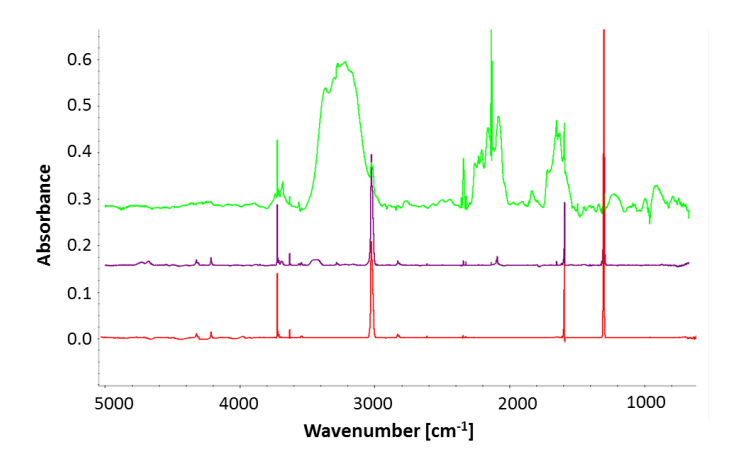
Ex situ electron microprobe measurements performed on the residues maintained under primary vacuum, show atomic $\frac{N}{N+C}$ ratio on the order of 0.5, supporting the hypothesis of formation of a HCN-like polymer.

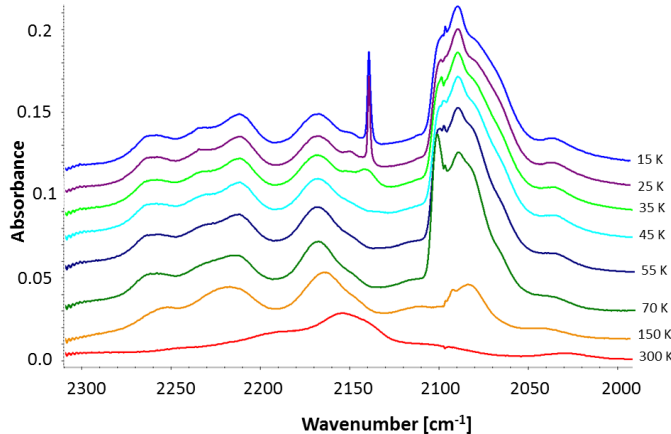
4.2. Comparison with UCAMMs

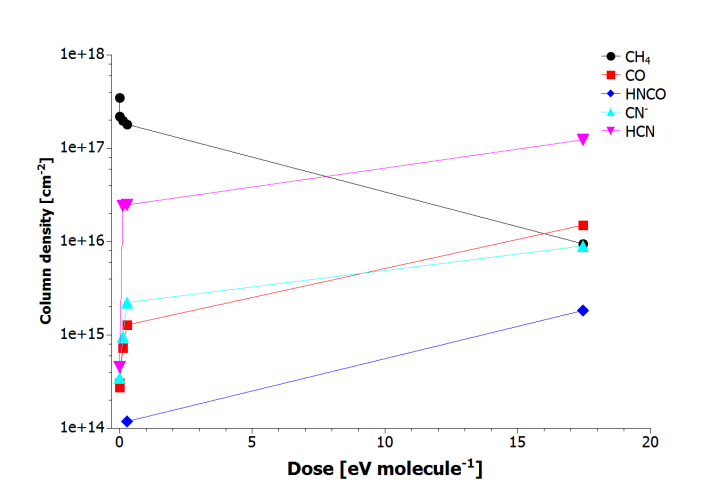
The residues obtained by irradiation of the above ice samples can be compared with the spectra of an UCAMM (Figure 9). The similarity between the spectra is striking, as the five major bands observed in the residues are also present in the UCAMM spectrum. There are still differences, such as the intensity of the nitrile and isonitrile region of the spectrum (2250-2100 cm⁻¹), which is more important in the residues. However, as shown in Figure 9 of Bonnet et al. (2015) and following the vacuum annealing at 300 °C of our residue from sample d, slight thermal evolution of the poly HCN and residue at T below about 300 K produces a better match to UCAMMs spectra. Thus the as-produced residues appear as meaningful precursors to UCAMMs.

4.3. Time scale

The present work allows to obtain constraints on the ability to produce the organic matter of UCAMMs or their precursors using simple processes ocuring in the Solar System. Furthermore







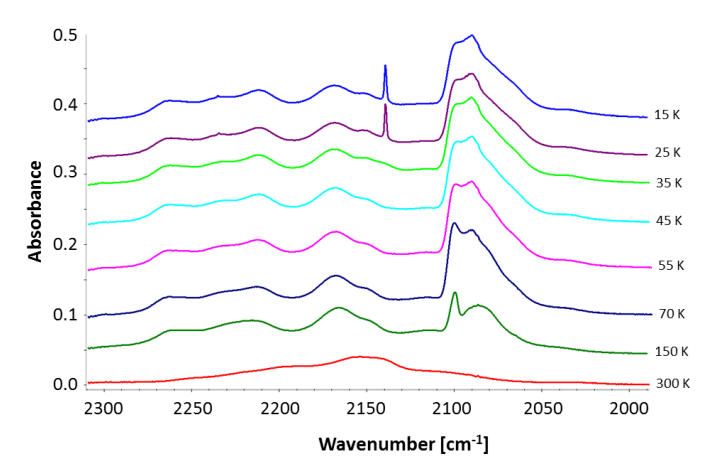


Fig. 6. (top) Sample d: IR spectrum from 5000 to 600 cm⁻¹ of N_2 :CH₄:H₂O (23 μ m thickness). From bottom to top, initial deposited ice sample (red) , after a fluence of 1.7×10^{11} ions cm⁻² (purple) and 2.2×10^{13} ions cm⁻² (green). The final dose is 18 eV molecule⁻¹. The final spectra indicates the presence of solid water, see text for details. Spectra have been shift for clarity. (bottom) Evolution of the column density of selected molecules in the sample during the irradiation as a function of the deposited dose. Due to a set-up problem, there is no point between 1 and 18 eV molecule⁻¹.

Fig. 7. (top) Evolution of IR spectra between 2300 and 2000 cm⁻¹ during annealing of sample a to 300 K. For a better reading, spectra have been shift. (bottom) Evolution of IR spectra between 2300 and 2000 cm⁻¹ during annealing of sample b to 300 K. Spectra have been shift for clarity.

they also allow to evaluate the associated time scales to form an UCAMMs precursor from the starting ice material. The cosmic ray dose experienced at large distances in the solar system can be evaluated by modeling their distribution and fluences (Shen et al. 2004, e.g.).

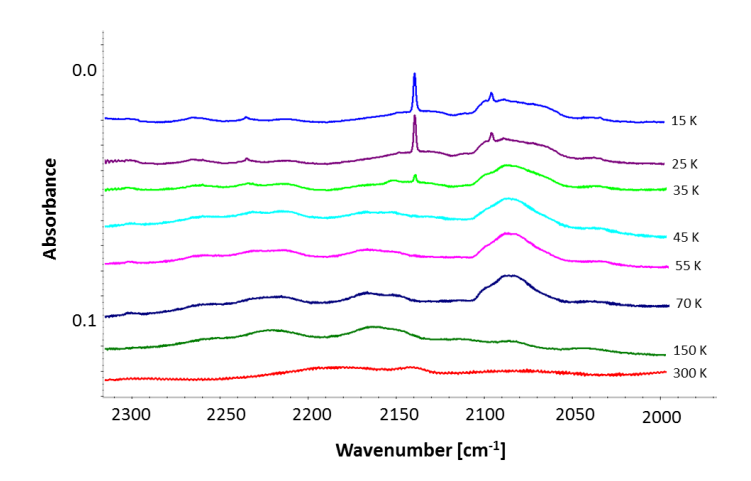
According to Cooper et al. (2003, Table 5), estimating with a model the times for accumulation of radiolytically significant dosages at the surface of icy bodies at large heliocentric distances and the local ISM, such an electronic dose can be deposited in and affect up to several μ m of ice layer. Although affecting only the top layer, such a process may produce substantial amount of organic matter in particular for small to intermediate sizes icy bodies in the Oort cloud.

The ice composition does not significatively change after a dose of 10-20 eV molecule⁻¹ (see Figure 4). The time corresponding to the deposition of this dose may therefore be considered as the time needed to produce an UCAMM precursor.

5. Conclusion

In the study reported by Shen et al. (2004) exploring cosmic rays interactions with icy grains, the mean rate of energy deposition to the ice mantles is of the order of 6×10^{-15} eV molecule⁻¹ s⁻¹. The equivalent time scale to reach an irradiation dose of about 10 eV molecule⁻¹ corresponds to about 53 million years, a dose at which an organic residue is already efficiently produced in the experiments presented in this work. This value represents a lower limit to the time needed to produce a solid organic matter precursor. Irradiating for longer times would produce more residues of similar nature (54 eV molecule⁻¹ corresponds to 270 millions years).

We performed irradiation with swift heavy ions of nitrogendominated ice mixtures of N₂-CH₄ (90:10 and 98:2) at 14 K, to simulate modifications induced by cosmic rays on transneptunian to Oort Cloud objects surfaces. During the irradiation, numerous intermediate species were produced, including predominantly HCN and CN⁻, but including also HNCO, CO or OCN⁻ from traces of water in the matrix. Starting from simple ice mixtures representative of icy surfaces of outer Solar System objects, we produce complex molecules and radicals. During the annealing of the irradiated ices to room temperature, these species recombine and react to produce a solid residue.



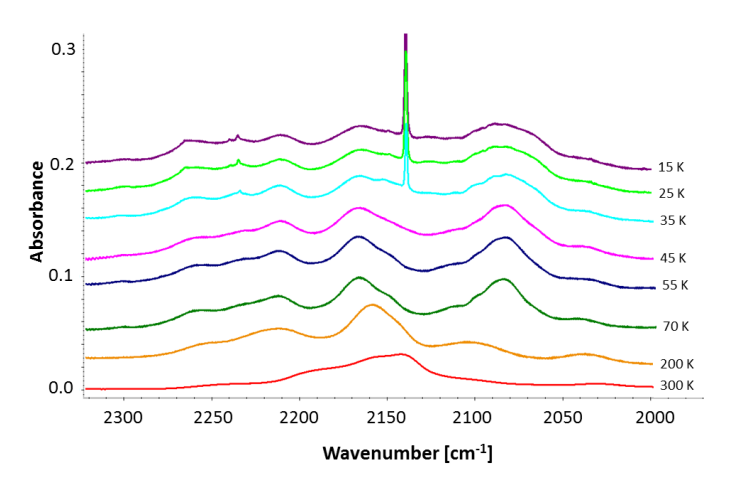


Fig. 8. (top) Evolution of IR spectra between 2300 and 2000 cm⁻¹ during annealing of sample c to 300 K. For a better reading, spectra have been shift. (bottom) Evolution of IR spectra between 2300 and 2000 cm⁻¹ during annealing of sample d to 300 K. Spectra have been shift for clarity.

The analysis of the residue confirm the formation of a poly-HCN like material, stable at room temperature. These poly-HCN like material are potential precursors of organic material observed in ultra carbonaceaous micrometeorites collected in Antarctica (UCAMMs). The associated formation time scale are compatible with an irradiation of icy bodies orbiting in the outer Solar System. Further studies should explore in detail the post irradiation of such residues when traveling to the internal parts of the Solar System.

Acknowledgements. This work was supported by the ANR IGLIAS project, grant ANR-13-BS05-0004 of the French Agence Nationale de la Recherche, by the CAPES-COFECUP French-Brazilian exchange program. MG, CE and JD acknowledge financial support from the ANR project OGRESSE (11-BS56-026-01) and DIM-ACAV. ED acknowledge financial support by the French INSUCNRS program "Physique et Chimie du Milieu Interstellaire" (PCMI). The Brazilian agencies CNPq (INEspaço) and FAPERJ are also acknowledged. We thank T. Been, C. Grygiel, T. Madi, I. Monnet, F. Ropars and J.M. Ramillion for their invaluable support.

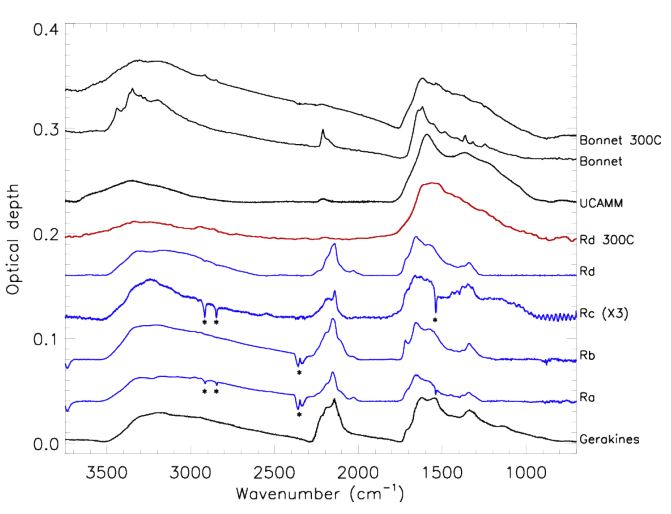


Fig. 9. Superposition of FTIR spectra of different residues compared to the spectrum of an UCAMM. From top to bottom: poly-HCN before and after annealing to $300\,^{\circ}\text{C}$ (Bonnet et al. 2015); spectrum of a UCAMM (Dartois et al. 2013); spectrum of residue "d" of this work, post-annealed to $300\,^{\circ}\text{C}$ (in red), spectra of residues "a" to "d" produded in this work after irradation and annealing to $300\,\text{K}$ (in blue); spectrum of pure HCN ice after irradiation (Gerakines et al. 2004).

References

Bennett, C. J., Jamieson, C. S., Osamura, Y., Kaiser, R. I. 2006, The Astrophysical Journal, 653, 792

Bentwood, R.M., Barnes, A.J., Orville-Thomas, W.J. 1980, Journal of Molecular Spectroscopy, 84, 391

Bonnet, J.Y., Quirico, E., Buch, A., et al. 2015, Icarus, 250, 53

van Broekhuizen, F.A., Keane, J.V., Schutte, W. A. 2004, Astronomy and Astrophysics, 415, 425

Burgdorf, M., Cruikshank, D.P., Dalle Ore, C.M., Sekiguchi, T. 2010, The Astrophysical Journal Letters, 718, L53

Cooper, J.F., Christian, E.R., Richardson, J.D., Wang, C. 2003, Earth Moon and Planets, 92, 261

Cruikshank, D. P., Grundy, W. M., DeMeo, F. E., Buie, M. W., et al. 2015, Icarus. 246, 82

Dartois, E., Engrand, C., et al. 2013, Icarus, 224, 243

Dobrică, E., Engrand, C., Leroux, H., Rouzaud, J.N., Duprat, J. 2012, Geochim. Cosmochim, 76, 68

Dobrică, E., Engrand, C., Quirico, E., Montagnac, G., Duprat, J. 2011, Meteoritics and Planetary Science, 46, 1363

Duprat, J., Dobrică, E., Engrand, C., et al. 2010, Science, 328, 742

Duprat, J., Engrand, C., Maurette, M., et al. 2007, Advances in Space Research, 39, 605

Ebihara, M., Sekimoto, S., Shirai, N., Tsujimoto, S., et al. 2013, Lunar and Planetary Science Conference, 44, 2086

Engrand, C., Benzerara, K., Leroux, H., Duprat, J., Dartois E., Bardin, N., Delauche, L. 2015, Lunar and Planetary Science, 46, 1902

Escobar, A., Giuliano, B. M., Muñoz Caro, G. M., Cernicharo, J., Marcelino, N. 2014, Astrophysical Journal, 788, 19

Gerakines, P.A., Bray, J.J., Davis, A., Richey, C.R. 2005, Astrophysical Journal, 620, 2240

Gerakines, P.A., Moore, M.H., Hudson, R.L. 2004, Icarus, 170, 202

Hudson, R.L., Moore, M.H., Gerakines, P.A. 2001, Astrophysical Journal, 550, 1140

Jheeta, S., Domaracka, A., Ptasinska, S., Sivaraman, B., Mason, N. J. 2013, Chemical Physics Letters, 556, 359

Licandro, J., Grundy, W. M., Pinilla-Alonso, N., Leisy, P. 2006, Astronomy and Astrophysics, 458, L5

Lorenzi, V., Pinilla-Alonso, N., Licandro, J. 2015, Astronomy and Astrophysics, 577, A86

Moon, E.S., Kang, H., Oba, Y., Watanabe, N., Kouchi, A. 2010, The Astrophysical Journal, 713, 906

Moore, M.H., Hudson, R.L. 2003, Icarus, 161, 486

Nakamura, T., Imae, N., Nakai, I., Noguchi, T., Yano, H., Terada, K. 1999, Antarctic Meteorite Research, 12, 183

Nakamura, T., Noguchi, T., Ozono, Y., Osawa, T., Nagao, K. 2005, Meteoritics and Planetary Science Supplement, 40, 5046

Palumbo, M. E., Strazzulla, G. 1993, Astronomy and Astrophysics, 269, 568

- Pilling, S., Seperuelo Duarte, E., da Silveira, E. F., Balanzat, E., et al. 2010, Astronomy and Astrophysics , 509, A87
- Satorre, M. Á., Domingo, M., Millán, C., Luna, R., Vilaplana, R., Santonja, C.
- 2008, Planetary and Space Science, 46, 1748
 Seperuelo Duarte E., Boduch P., Rothard H., Been T., Dartois E., et al. 2009,
 Astronomy and Astrophysics, 502, 599
- Shen, C.J., Greenberg, J.M., Schutte, W.A., van Dishoeck, E.F. 2004, Astronomy and Astrophysics, 415, 203
- Yabuta, H., Itoh, S., Noguchi, T., et al. 2012, Lunar and Planetary Science Conference, 43, 2239
- Ziegler, J. F., Ziegler, M. D., Biersack, J. P. 2010, Nuclear Instruments and Methods in Physics Research B, 268, 1818